Published in final edited form as:
J Vasc Interv Radiol. 2009 October ; 20(10): . doi:10.1016/j.jvir.2009.06.029.

Cryotherapy for Breast Cancer: A Feasibility Study without Excision

Peter J. Littrup, MD, **Bassel Jallad, MD**, **Priti Chandiwala-Mody, DO**, **Monica D'Agostini**, **Barbara A. Adam, BSN**, and **David Bouwman, MD**
Department of Radiology, Karmanos Cancer Institute, 721 Harper Prof. Bldg Detroit, MI 48201 (P.J.L., B.J., M.D., B.A.A.); and the Departments of Radiology (P.C.M.) and Surgery (D.B.), Wayne State University, Detroit, Michigan

Abstract

PURPOSE—To assess the feasibility of percutaneous multiprobe breast cryoablation (BC) for diverse presentations of cancers that remained in situ after BC.

MATERIALS AND METHODS—After breast magnetic resonance (MR) imaging and thorough consultation, patients underwent BC after giving informed consent. This study was approved by the institutional review board. In 12 BC sessions, 22 breast cancer foci (stages I–IV) were treated in 11 patients who refused surgery by using multiple 2.4-mm cryoprobes. Five patients had recurrent disease and six had new diagnoses. With use of only local anesthesia, six patients were treated with ultrasonographic (US) guidance and five were treated with both computed tomographic (CT) and US guidance. Saline injections and warming bags were used to protect the skin. Procedure success was defined as 1 cm visible ice beyond all tumor margins. MR imaging and/or clinical follow-up were available for up to 72 months after BC.

RESULTS—US produced sufficient ice visualization for small tumors, whereas CT helped confirm overall ice extent. The mean pretreatment breast tumor diameter was 1.7 cm ± 1.2 (range, 0.5–5.8 cm), and an average of 3.1 cryoprobes produced 100% procedural success with mean ice diameters of 5.1 cm ± 2.2 (range, 2.0–10.0 cm). No significant complications, retraction, or scarring were noted. Biopsies at the margins of the cryoablation site immediately after BC and at follow-up were all negative. No local recurrences have been noted at an average imaging follow-up of 18 months.

CONCLUSIONS—In conjunction with thorough pre- and postablation MR imaging, CT/US-guided multiprobe BC safely achieved 1 cm visible ice beyond tumor margins with minimal discomfort, good cosmesis, and no short-term local tumor recurrences.

Breast conservation is a major goal of cancer treatment, and local excision (ie, lumpectomy) followed by radiation therapy is the current standard of care. However, 35% of patients who undergo lumpectomy note serious breast asymmetry, and morbidity rates of 11% for bleeding and 3% for infections (1). Therefore, many different minimally invasive options have been considered, including thermal breast ablation techniques such as radiofrequency, high-intensity focused ultrasonography (US), microwave, interstitial laser, and cryoablation (2). Nonthermal techniques, such as irreversible electroporation, may also hold promise due to minimal scar formation. However, irreversible electroporation has not been clinically

Address correspondence to: P.J.L.; littrupp@karmanos.org.

None of the other authors have identified a conflict of interest.

used for breast cancer and currently requires general anesthesia and paralysis to avoid severe muscle contractions (3).

Nonsurgical localized tumor eradication may have even greater relevance in the era of improved magnetic resonance (MR) evaluation and guidance (4). MR imaging has become the gold standard for breast cancer screening of high-risk women (5,6) but may also have 90% sensitivity for detecting the premalignant or co-existing condition of high-grade ductal carcinoma in situ (DCIS) (7,8). Autopsy series suggest that not all DCIS is clinically relevant (9), nor does it always progress in the contralateral breast if undetected or left untreated (10). MR imaging thus has exceptionally high negative predictive value to exclude the presence of all clinically relevant tumors if ablation is to be considered for eradication of the dominant tumor(s). Techniques and utility of MR imaging for biopsy and guidance have also been established (11). Nevertheless, equipment compatibility and access to interventional MR units make computed tomographic (CT) and/or US guidance the preferred method for guiding ablation in most organ sites. Careful US targeting of MR imaging findings has been described (12,13), as has the potential for MR biopsy to leave a range of clips that are visible at US (14).

Cryoablation is the best visualized of all ablation techniques due to the phase change during ice formation. The margins of low-density, solid ice are well seen with US, CT, and MR imaging (4,15–27). Considering its lower procedural pain (20), cryoablation may have unique benefits for cost-effective out-patient breast cancer therapy using only local anesthesia and/or mild sedation. The greater resorption of the cryoablation zone than heat-based ablations (18,22) also fulfills cosmetic goals. However, thorough cryoablation of any breast cancer is paramount over breast conservation and requires the generation of lethal isotherms throughout a tumor(s) by using well-established multiprobe placement considerations (15–18). Indeed, under-treatment and local recurrence rate of 38% within 6 months can occur if only two cryoprobes are used for tumors as large as 5 cm, despite MR visualization of tumor coverage by ice (21). US-guided breast cryoablation (BC) has shown encouraging results for benign disease (22,23) but only limited application for cancer. Unfortunately, BC reports for cancer used only a single cryoprobe and concluded that BC was insufficient for treating breast cancers larger than 1.5 cm (24–26).

Combined with thorough preoperative MR tumor evaluation, the well-visualized ablation zone of ice could thus be sculpted under direct US and/or CT guidance to cover one or more tumor foci with use of several cryoprobes (15–20). We assessed the feasibility and initial outcomes of percutaneous multiprobe cryoablation for diverse presentations of in situ breast cancer, emphasizing 1 cm visible ice coverage beyond all tumor margins.

MATERIALS AND METHODS

Patient Aspects

Patients were treated between April 2003 and October 2008. Eleven patients who presented for BC had undergone biopsy and were diagnosed with cancer before their consultation in our multi-disciplinary comprehensive breast center. Women who refused any surgical options for breast cancer, clinical stage A through D (Table), were considered for cryoablation if they were still willing to comply with recommendations of radiation therapy and/or chemotherapy–hormonal therapy following ablation as appropriate. Patients were considered in two main groups: those receiving cryoablation for the control of locally advanced or recurrent disease and those in whom cryoablation was part of their treatment regimen for their primary cancer (ie, “Recurrent” and “New Dx,” respectively, Table). The latter group could be considered as receiving BC for potential cure, in conjunction with probable radiation therapy and/or chemotherapy–hormonal therapy. If patients had apparent

localized disease, they had to agree to sentinel lymph node dissection before cryoablation. In this manner, cryoablation was at least considered a better local treatment than no local debulking at all. Inclusion criteria was intended to assess our hypothesis that approximately 1 cm of visible ice could be safely generated around all visible margins of tumor regions up to 7 cm in patients refusing surgical resection. A 1-cm ice margin serves as a conservative estimate of cytotoxic temperatures throughout the tumor (15–18,22) and recently has been validated by body-temperature phantoms for multiple cryoprobes (27). Exclusion criteria included tumor skin involvement, uncorrectable bleeding diatheses, inability to give consent, and tumor regions not feasibly covered by up to eight cryoprobes, including outer distances between multiple tumors (eg, 7 cm). Following thorough consultation and MR staging, informed consent was then obtained and patients were followed in compliance with our institutional review board–approved protocol for general ablation and Health Insurance Portability and Accountability Act regulations.

Staging/Imaging Aspects

MR images were obtained at our institution if a patient did not present with a recent dynamic contrast medium–enhanced breast MR image of comparable quality within the last 6 weeks. Women underwent imaging at our center with a 1.0- or 1.5-T unit (Harmony; Siemens, Erlangen, Germany) by using standard sequences before and after the intravenous administration of gadolinium (0.1 mmol/kg Magnevist; Berlex Laboratories, Wayne, New Jersey). A half-Fourier rapid acquisition with relaxation enhancement (flip angle, 150°; section thickness, 5 mm with 30% gap) was used for T2-weighted imaging. A fat-suppressed, T1-weighted, axial, volume-interpolated breath-hold technique (ie, VIBE = 5.12/2.51; flip angle, 10° section thickness, 2.5 mm) was used at 0 minute, 45 sec, and 2 and 3 minutes after contrast medium injection.

A high-frequency (10–13 MHz) linear-array US transducer (Logiq 700; GE Medical Systems, Milwaukee, Wisconsin) was used to document breast cancer sizes, guide thermocouple and cryoprobe placements, monitor iceball formation, and guide safety measures of sterile saline injections. MR evaluation of tumor extent, cryoablation planning, and US monitoring were performed by a certified breast radiologist (P.J.L.) with approximately 15 years of experience in breast imaging, US guidance, and ablation. Each breast cancer was characterized with respect to its location within the breast and its width, height, and length. US guidance was used in all patients. Five patients (six of 12 procedures) also received concomitant CT guidance. These six CT-guided BC procedures were predominantly used in the group of patients with recurrent disease with bulky or multifocal tumors, as well as in the last two newly diagnosed patients with multifocal tumors for better circumferential visualization of ice coverage.

CT of the chest and abdomen was done before BC for the staging of patients with recurrent disease (Table). CT documentation of ice progression during the procedure relied on intermittent CT fluoroscopy, requiring exposures of 70 mA and 120 kV for this older scanner (Somatom Plus4 and Care-Vision fluoroscopy package; Siemens). Helical scans having less quantum mottle (280 mA and 120 kV) were obtained for greater clarity at the completion of the first and second freeze cycles. Multiplanar reconstructions were used after the first freeze to assess initial tumor margins in relation to probe distribution and ice margins. If the visible ice margin did not extend beyond all apparent tumor margins, an additional cryoprobe was placed during the thaw phase at that site or probes were repositioned. CT images of final ice dimensions in transverse, anteroposterior, and cranio-caudal dimensions were recorded from helical scans obtained immediately after probe removal, thereby eliminating beam-hardening artifact from the cryoprobes.

Cryoablation Aspects

During the course of this study, 2.4-mm-diameter cryoprobes (Endocare, Irvine, California) were used. The cryoprobes had straight or right-angled shafts, but identical performance characteristics, and were approved by the U.S. Food and Drug Administration. Both types of cryoprobes contain a Joule-Thompson port at the distal end and have active freeze lengths of 4 cm, generating individual ice of 2.5 × 4.5 cm in room-temperature phantoms (27). The cryoablation control unit has up to eight ports (Endocare) regulating the flow of high-pressure argon gas. Helium gas was used to actively thaw the cryoprobes immediately after completion of the second freeze cycle, which generally took approximately 2 minutes until cryoprobes were movable and could be withdrawn.

The general BC procedure will be described first, followed by specific procedure modifications. Only the first patient received general anesthesia due to concurrent sentinel lymph node dissection. All subsequent breast cancer patients received local anesthesia and minimal sedation as needed during the procedure, with the following ranges: diphenhydramine hydrochloride, 25–50 mg; morphine, 2–10 mg; and/or midazolam, 1–8 mg. An experienced radiology nurse (B.A.) monitored levels of consciousness, oxygenation, hemodynamics, and the visual analog scale for pain, administered moderate sedation, and contacted patients for postablation clinical follow-up. Intravenous antibiotic prophylaxis (eg, cefazolin sodium,1 gm) was routinely administered before cryoablation. Patients were prepared and draped in sterile fashion. The angle of approach was chosen along the longest axis of the breast tumor(s) to better utilize the longer freeze length of the cryoprobe. A lateral or inferior puncture site was selected when possible to optimize cosmetic results. The overlying skin was infiltrated with buffered 1% lidocaine. Deeper tissues surrounding all tumor margins were infiltrated with 2% lidocaine containing 1:100,000 epinephrine. The center of the tumor was first targeted with a 20-gauge spinal needle. For patients requiring biopsy, a trocar needle (Coaxial Biopsy Needle [C1816A]; C.R. Bard, Covington, Georgia) was placed with its tip at the leading edge of the tumor in preparation for subsequent core samples.

At least two cryoprobes were placed parallel to the central needle according to Figure 1, and this accounted for the greater heat-sink effect along the posterior margins (Fig 1b). Multiple cryoprobes were placed approximately 1.5 cm apart and less than 1 cm from all tumor margins according to established guidelines for generating cytotoxic isotherms in almost any tissue (15–18). For the relatively low heat load of breast tissue compared to internal organs, it was assumed that 1 cm of visible ice beyond all tumor margins would generate cytotoxic temperatures (eg, ≤30°C) throughout the tumor (27). Total probe number was projected to be more than the tumor diameter in centimeters. For example, a 4-cm tumor or two tumors within a 4-cm area would require a minimum of four cryoprobes to generate a 6-cm-diameter iceball that overlapped all tumor margins by 1 cm. Cryoprobes were advanced through the breast cancer so that the tip extended just beyond the tumor margin. Transverse US helped confirm probe distribution, and longitudinal scanning helped confirm placement of the tip just beyond the distal tumor margin (Fig 2).

Safety and visual control criteria of 1 cm of ice beyond tumor margins determined the extent of the freeze protocol segments, causing variable freeze cycle times. The first freeze cycle was continued until the visible ice extended more than 5 mm beyond the apparent tumor margins, lasting between 5 and 13 minutes (average, 9.3 minutes) depending on tumor size and cryoprobe distribution (ie, spacing and number). A 5–10 minute thaw phase (average, 8.1 minutes) followed, whereby the probes were placed to a ‘stick’ setting that kept them fixed within the tissue but not actively cooling. Any needle adjustments for skin infiltration or to prepare warmed sterile saline bags generally determined variations in thaw time. The second freeze cycle was continued until visible ice extended beyond the original ice extent

or approximately 10 mm beyond all apparent tumor margins. Due to the fourfold greater thermal conductivity of solid ice than tissue liquid (28), the second freeze rapidly recooled the ice volume (22,27) and allowed refreeze times of 4–10 minutes (average, 7.3 minutes). The second freeze time was also shortened as needed to control skin safety.

Protection of adjacent crucial tissues from freezing temperatures was achieved with injected saline (18,22) and/or by placing warm sterile saline bags directly on the skin surface (eg, 250-mL bags placed in a microwave for 40 seconds). Sterile saline injections (range, 10–100 mL) were used throughout both freeze cycles to widen the space between the iceball and the skin surface or, to a lesser extent, the chest wall. If the tumor was 0.5–1.0 cm from the skin surface, injected saline was usually sufficient. If the tumor was less than 0.5 cm from the skin surface, warmed saline bags were also used because they helped keep the epidermis soft for continued saline injection throughout the procedure.

Chest wall structures were generally protected by anterior elevation of the entire cryoprobe(s), thus retracting the developing ice away from the chest wall (18,22,23). Gentle to-and-fro movement of the iceball during anterior retraction also prevented ice from adhering to the underlying pectoralis muscle. After the second freeze cycle, cryoprobes were removed, peri-ablational biopsies were performed (noted below), and manual pressure was applied for 10–20 minutes. If saline had been used during treatment, the patient was counseled on the greater probability of continued serosanguinous drainage during the first 24 hours. An absorptive bandage was applied and the patient discharged within 2 hours. However, patients were told to avoid tape if possible by simply using absorptive pads (eg, menstrual pads) inside their brassiere for the first few days as needed.

Additional diagnostic needle biopsies of breast tumors during cryoablation (eg, confirming outside pathology or if additional samples were requested) were delayed until the first freeze cycle was ready to be initiated to minimize bleeding that could have obscured cryoprobe placement. A 14-gauge automated needle (Maxcore Biopsy Instrument [MC1416]; C.R. Bard, Covington, Georgia) was used to obtain two to three cores for histologic examination. In patients being treated for potential cure (“New Dx,” Table), the problem of subclinical tumor or DCIS beyond the ablation margins was addressed in part by performing 14-gauge biopsies from the superior, inferior, medial, and lateral margins of the final iceball. These were simply done with combined palpation guidance of the ice edge along with US guidance to confirm the safety of the needle trajectory. The anterior and posterior margins were generally too close to the skin surface or were too deep to the iceball along the poorly visualized chest wall to be sampled, respectively.

Specific BC procedure modifications were needed for some patients with diverse tumor sizes and locations. These technique variations are described, but the BC goal of delivering cytotoxic temperatures throughout the tumor by extending visible ice 1 cm beyond all apparent tumor margins remained the same. The multidisciplinary team recommended microlumpectomy sampling for our first BC patient to debulk visible tumor and provide additional pathology specimens by using an 11-gauge US-guided Mammotome (Ethi-con Endo-Surgery, LLC, Cincinnati, OH) immediately before cryoablation. Two cryoablation probes were then placed along the outer margins of the two residual Mammotome cavities while a third probe was placed in the intervening tissue to maintain 1.5-cm probe separation. Thermocouples were used in two patients to ensure cytotoxic ice formation. A thermocouple was placed in our second patient according to a previously described technique (22) because the tumor was too large to contemplate a microlumpectomy approach. Due to the added procedural complexity, thermocouples were then only used in a later patient with multifocal recurrence to document cytotoxic temperatures between different portions of the large

confluent ice (Table, patient 9). One patient with bulky disease (Patient 4, Table; Fig 3) had breast implants.

Follow-up

Patients were discharged home after confirmation of stable vital signs and managed their discomfort with only nonnarcotic analgesics (eg, acetaminophen for the first 2 days and then ibuprofen). A pain scale questionnaire was assessed with a 24-hour follow-up phone call. A numeric rating pain scale was used, corresponding to a range of 0 (no pain) to 10 (severe pain). Treatment-related adverse events were noted according to both the Common Toxicity Criteria for Adverse Events Version 3.0 (CTCAEv3) of the National Cancer Institute (29) and the Society of Interventional Radiology (SIR) classification system (30). The CTCAEv3 has more complication-specific details related to outcomes and therapeutic responses. The following generalizations were used to classify major and minor complications: Major complications were classified as CTCAE grade 3 or more or SIR grade C–F, and minor complications were classified as CTCAE grade 1–2 or SIR grade A–B. At the latest clinical contact, as noted in the Table, patients were also asked to rate their satisfaction with the procedure as very happy, somewhat happy, ambivalent, disappointed, or very disappointed.

Follow-up imaging included routine contrast-enhanced chest and abdomen CT for staging patients with recurrent disease at 3, 6, and 12 months, as available. Breast MR imaging was performed in all women who underwent BC at 1, 3, 6, 12, 18, and 24 months and yearly thereafter. Clinical follow-up was limited to telephone contact for out-of-state patients (n = 9), who were requested to send copies of available MR images. Imaging follow-up time was noted from the last available breast MR image, whereas clinical follow-up extended from the time of cryoablation to our latest phone contact or clinic visit. Any ablation size increase or distinct development of asymmetric and/or nodular enhancement was considered suspicious (30) and biopsy confirmation recommended by best visualized approach. After biopsies of minor ablation rim asymmetries revealed only inflammatory changes at 6 weeks in our first patient, we limited a suspicious abnormality to a nodular aspect larger than 5 mm. Enhancement kinetics were also evaluated according to standard parameters (CADstream System; Confirma, Kirkland, Washington) before biopsy recommendation.

Patient data consisted of tumor and ice diameters (Table), 24-hour postprocedure pain scores, postablation imaging evaluation, biopsy outcomes, and telephone interview of level of patient satisfaction. Immediate procedural success was defined as coverage of all tumor margins by 1 cm of visible ice. Due to limitations of shadowing from the leading edge of the ice during US guidance, this 1-cm margin had to be defined in relation to adjacent landmark structures 1 cm beyond the well-visualized tumor margins. Short-term local success in follow-up was defined as no evidence of suspicious enhancing nodularity (ie, >5 mm) of the ablation margin that could be confirmed at biopsy and/or no continued mass progression on further follow-up images. Due to the small sample set, no comparative statistical analyses were performed to assess the significance of data parameters. The study was not powered to assess any specific feasibility aspects and is limited to descriptive statistics.

RESULTS

Patient Aspects

The average patient age was 62.5 years. All patients tolerated BC procedures as outpatients, with only two patients requesting mild sedation for anxiety before the procedure. More frequent wound oozing was noted than in our fibroadenoma series (22,23), and some patients required several bandage changes in the first 24 hours, particularly if they received saline injections. Injected saline of up to 100 mL for skin protection allowed the generation

of 1-cm ice ablation margins beyond all tumor margins, even if the tumor was within 1–2 mm of the skin surface. Bruising and breast edema (grade 1/2) were common for all women but required no drainages or interventions. The average procedure discomfort at 24 hours was 0.3 on the 10-point pain scale (range, 0–4), with only two patients not being contacted due to their out-of-state travel status. The patient with the highest pain score of 4/10 was well controlled with analgesics and had been 3/10 before the-procedure due to the subcutaneous/sternal tumor recurrence (patient 8, Table). Her pain subsequently completely resolved by 1 month, and she remains tumor- and pain-free at 37-month follow-up. No skin necrosis was noted and no complications of grade 3 or higher were identified. Patient satisfaction of “very happy” was noted in 10 of 11 patients; follow-up contact data could not be obtained for one out-of-state patient.

Procedural Imaging Aspects

In this study, 22 breast cancer foci in 11 patients were treated in 12 cryoablation procedures. This included four nodes within the axilla as separate ablation sites. The average tumor size (±standard deviation) was 1.7 cm ± 1.2 (range, 0.5–5.8 cm; Table). US guidance was sufficient for smaller tumors that were well seen (Fig 2) and did not lie deep within the breast. For deep masses and those requiring at least three cryoablation probes, the circumferential ice visualization with CT provided greater assurance of thorough coverage, particularly along the posterior tumor margin (Fig 3). CT definition of low-density ice extending beyond all tumor margins could be well seen in fatty breasts or if the mass resided in a more fatty region of a breast with scattered density. However, a cancer residing within dense breast parenchyma precluded CT guidance of cryoprobe placement and monitoring of ice progression, whereby US guidance was used despite its own limitations with posterior shadowing. For US guidance, the posterior margins were always obscured, and retracting the breast mass off the chest wall helped prevent ice progression into the underlying chest wall with minimal need for posterior saline injection (Fig 2b). With the exception of patient 9 (Table), who underwent only US guidance due to a technical malfunction of the CT scanner, all BC procedures for recurrences, multifocal tumors, and axillary lesions were performed with CT/US guidance to obtain the best combined visualization.

Cryoablation Aspects

The average number of cryoprobes used per patient was 3.3 (range, 2–7 probes), with a mean ice ball diameter of 5.1 cm ±2.2 (range, 2.0–10.0 cm). This produced 100% procedural success as noted from tumor margin coverage by approximately 1 cm of visible ice. However, visualization of the ice margin to the underlying tumor could not be clearly distinguished for all US-guided cases as well as for CT guidance in patients with dense breasts. The 1-cm margin, therefore, was estimated from adjacent landmark structures within the breast and further validated with subsequent follow-up MR imaging on the basis of avascular ablation zones and similar estimated volumetric landmarks. Thermocouples proved cumbersome and were only used to document cytoxic temperatures in two cases. The lowest temperature noted near the tumor margin and approximately 7 mm from the nearest cryoprobe was −57°C (Fig 2a) (patient 2, Table). The thermocouple along another ice margin where two axillary tail masses abutted the confluent ice from the supraareolar lesion reached −37°C (Table, patient 9). The six patients who underwent biopsies at the time of BC showed no cancer or DCIS from the regions sampled adjacent to the final iceball. The five patients who did not undergo paraablational biopsies received cryoablation for local control of recurrence.

The most technically challenging aspect of BC was maintaining vigilant control of the ice margin near the skin surface to prevent full-thickness necrosis. Generous saline injection was needed before the ice came within 5 mm of the skin surface. If ice proceeded too

quickly to the skin surface, it was more difficult to inject against the pressure of the underlying hard ice. Warmed bags of sterile saline helped prevent hard ice from penetrating through the skin, but the more anterior probes also needed to be turned down (eg, 10% flow) to maintain control. Vigorous rubbing of the overlying skin with the saline bags also helped prevent full-thickness skin freeze.

Follow-up

The average length of clinical follow-up was 22.8 months, with an average imaging follow-up of 17.5 months. Unfortunately, this included three patients with no additional contact such that, for the patients with available data, the clinical follow-up was 25.2 months, with an average imaging follow-up of 23.0 months. Because most patients were out of state, we had to rely on available imaging protocols of local facilities; however, all outside studies employed dynamic contrast-enhanced MR imaging. The imaging course of ablation sites followed the same relative pattern seen after ablation in other sites (4,15–20,22,23,31). Within the first few days, residual blood flow within tumors is nonspecific if the ablation margin extends well beyond the site. From 1 to 12 weeks, a symmetric thin rim of enhancement can be seen surrounding the otherwise avascular ablation volume. No patient had progressive asymmetry or an increase in nodular enhancing margins on repeat images. In addition, patients generally preferred to delay biopsy decisions until follow-up breast MR imaging 3 months later confirmed persistent nodularity or its enlargement. To date, no progressive nodularity has been seen on breast MR images.

The greatest reduction in ablation volume occurred between 3 months and 2 years (18,19,22,23) but was not calculated for our limited patient group with variable imaging parameters in follow-up. Figure 3 demonstrates 95% volume reduction in ablation volume (65.1 vs 4.1 mL) by 22 months (patient 4, Table), compatible with other cryoablation healing patterns (1,2,9,10). This patient also had near-complete resorption and minimal scarring around the ablation sites covering the recurrent cancer foci in the axillary node and small upper breast nodule. No apparent deleterious effects on the underlying breast implant were noted. She remains very pleased with breast pain relief (currently 0/10), lack of cancer recurrence following the second cryoablation, preservation of her implants, and cosmetic outcome (Fig 4). Another patient with 3-year CT follow-up (Fig 5) had a 4.2-cm sternal soft tissue recurrence (patient 8, Table) that came within 1 mm of the skin surface but showed 93% post-BC reduction and a thin scar (28.0 vs 1.9 mLc). Even if only the superficial soft tissue component was considered, 87% reduction was still noted and she has remained free of local or distant recurrences over 3 years. All other patients reported similar satisfaction with long-term cosmetic appearance and minimal residual palpable mass effect.

The two patients who underwent biopsy 6 weeks after cryoablation also showed no residual cancer or DCIS. Tissue from abscess débridement 4 years after cryoablation in our first patient (Fig 4) was also negative for tumor or DCIS. The patient with breast implants (Fig 3) had negative biopsies from the dominant ablation sites 6 weeks after BC, including negative cytology from the subareolar component that had undergone liquifactive necrosis. Her subsequent biopsies of the two new suspicious findings beyond the ablation site at 7 months revealed DCIS with micro-invasive cancer in a new axillary node and invasive adenocarcinoma in the small, upper breast mass. Following repeat cryoablation of these additional foci, she remains disease-free in the breast and axilla at 22 months despite slow progression of her bone and pulmonary metastases.

DISCUSSION

Our clinical experience with multi-probe BC for a broad clinical presentation of breast cancer suggests that cyto-toxic isotherms can be accurately predicted and controlled. Large

treatment zones appeared to thoroughly destroy bulky tumors and/or multifocal disease in almost any location within the breast, resulting in marked resorption of the ablation zone and minimal scarring. Pre-BC MR evaluation helped plan the extent of freeze margins and the number of probes required and identified additional cancer foci to include in the ablation zone. BC was well-tolerated in an outpatient setting, similar to cryoablation for benign breast masses (22,23), despite the use of several cryoprobes and concurrent biopsies. The combined use of saline injection and warming bags was needed to prevent skin damage, yet facilitated the aggressive ablation goal of extending visible ice 1 cm beyond all apparent tumor margins. Our 100% procedural and local short-term success rate is encouraging for further nonsurgical, in situ evaluations of BC.

Our experience with cryoablation for breast cancer is different from that described in all other BC publications. Previous investigators used only a single cryoprobe for breast cancers up to 1.5 cm (3–5), but we also did not resect the cryoablation site and monitored long-term healing, demonstrating minimal breast distortion and no local cancer recurrence. Our experience with cytotoxic principles for covering tumors up to 7 cm in many tissues (15–19,22,23) gave us confidence in providing aggressive local ablation, especially because our patients refused any surgical option. We acknowledge that extensive work with cytotoxic isotherms for prostate cancer (16,17) and other articles showing the importance of at least two probes for almost any organ (15) may not seem applicable to cryoablation for breast cancer. However, the heat load in breast tissue is probably less than that for any internal organ. Indeed, as long as multiple cryoprobes are used in conjunction with accurate treatment planning with breast MR imaging, reliable cytotoxic isotherms appear possible without thermocouples by simply extending CT/US-visible ice more than 1 cm beyond all tumor margins.

Cryobiology in breast tissues was first addressed by Rand et al (32), who showed that cryotreatment before resection decreased local tumor recurrence by 70% in an animal model. Hong and Rubinsky (33) then defined the mechanisms of in vitro ice propagation within normal and malignant tissues. Staren et al (34) extended their work by detailing cryotoxicity parameters in an animal model with the first human treatment. Rui et al (35) provided freeze protocols that generated thorough in vitro cytotoxicity for both normal and cancerous cells whereby a double freeze-thaw cycle ensured complete cell destruction, either for a target temperature of −40°C using a 25°C/min cooling rate or a −20°C target for a 50°C/min faster cooling rate. In other words, if the periphery of a tumor measured −20°C after freezing 1 minute or −40°C after 3 minutes, complete cell kill may be safely assumed. This corresponds to a 57°C drop in temperature from ~37°C to −20°C within 1 minute for a cooling rate greater than 50°C/min or a 77°C drop in temperature from ~37°C to −40°C after 3 minutes for a cooling rate greater than 25°C/min. Freeze rates from our fibro-adenoma study (22) were estimated to be between 10° and 25°C/min by using a single probe at the periphery of masses smaller than 2 cm, but could have been pushed to more than 25°C/min with closer placement of cryoablation probes in a denser probe configuration according to tumor size (16–18). If we use a target temperature of −40°C and a total freeze time of 15 minutes, the 77°C drop in temperature from 37°C to −40°C produces a freeze rate of only ~5°C/min. Therefore, the faster we can deliver cytotoxic temperatures throughout a tumor by using multiple cryoprobes, the greater the likelihood of complete cell kill.

We are confident that our multi-probe freeze approach contributed to our 100% local success rate at 18 months. This likely produced an intra-tumoral freeze rate of more than 15°C/min for the first freeze and more than 25°C/min for the second freeze, which was an average of 2 minutes shorter. Detailed freeze rate factors were not fully considered by Phleiderer et al (24,26) in reporting human breast cancer cryotoxicity. Lumpectomy specimens were obtained 5 days after cryoablation from 15 patients with 16 breast cancers

averaging over 2 cm. They reported only temperatures from within a single cryoprobe, thus limiting cooling rate estimates to only a few millimeters from the cryoprobe (~100 °C/min). Nevertheless, five of their patients with tumor diameters less than 16 mm showed complete destruction of the invasive tumor component with use of only a single probe. Of these five patients, two showed DCIS in the vicinity of the cryosite. They also concluded the need for multiple cryoprobes, especially for tumors larger than 16 mm, which showed incomplete treatment along the posterior margins.

Several aspects of our limited series highlight the benefits of multiprobe BC in the overall trend toward greater breast conservation. We treated a spectrum of women at high risk for localized recurrence, from multifocal initial presentation to bulky local disease recurrences (Table). We were able to generate aggressive freeze profiles for larger regions almost anywhere in the breast by using equally aggressive skin protection measures. Cryoablation appears much more flexible than radiofrequency limitations of 1 cm away from skin or chest wall (36), which may still cause skin puckering (37) or produce high cancer recurrence rates (38). Perhaps more important, we have also noted that cryoablation ablation zones resorb much better than previous descriptions of radiofrequency ablation zones (18). Cryoablation thus has distinct benefits over heat-based ablations by thorough resorption of the ablation zones, leading to minimal mass effect by 12–18 months, which is both palpably and cosmetically appealing to patients (Figs 3–5). It is also uncertain whether breast implants could tolerate heat sufficient for ablation. Despite the initial bruising when ice came close to the skin surface, the cosmetic outcome after several months was proportionate to the volume loss of the resorbed, smooth ablation zone and showed no retraction or apparent underlying scarring. Patients described gradual softening of the palpable ablation zone for several months, similar to the healing noted with the smaller cryoablations for fibroadenomas (22). However, even accidental cryoablation zone progression into the chest wall does not appear particularly deleterious because the iceball was deliberately driven into the chest wall for thorough tumor coverage within the sternum (patient 8, Table, Fig 5). Nevertheless, retraction of the iceball away from chest wall is quite effective to prevent unnecessary damage to pectoralis musculature.

Our study also is also unique in showing technical success with ablation of four separate malignant axillary nodes by using combined US/CT guidance. These were limited to an enlarged suspicious node but could conceivably treat almost any visible group of nodes (eg, likely <4 nodes), assuming sufficient safety considerations. We caution against the use of cryoablation in the axilla unless the course of the major nerves to the arm (ie, brachial, ulnar, radial) are anatomically defined in relation to the node and motor testing of the hand is also done intermittently throughout the freeze. The low pain of cryoablation also allows BC to be performed more readily in a conscious patient. We have used the following commands during other chest wall ablations that come close to the brachial plexus: “make a fist” (brachial nerve), “make a stop sign” for dorsiflexion of the wrist (ulnar nerve), and “make an O.K. sign” (radial nerve). Further work is also needed for percutaneous axillary node sampling for concurrent tissue confirmation at the time of ablation, particularly in women desiring to completely avoid axillary lymph node dissection following positive sentinel node biopsy.

Controversies about BC (39) may need further consideration as rapid technologic advances continue to affect diagnosis and staging. Major treatment decisions for additional chemotherapy and/or radiation therapy after lumpectomy currently depend on knowing the tumor size from the resection specimen. We agree that estimation of tumor size may be less accurate with US or MR imaging, but histologic tumor measurements may not remain as a practical “gold standard,” especially for smaller tumors. Breast specimens also have variability due to tumor and tissue shrinkage during fixation (40,41). Distortion of specimen

tumor measurements after large-core breast biopsies obtained with vacuum-assisted devices are even more likely for small tumors (42). Tumor measurements from lumpectomy specimens are thus unreliable when very little or even no residual tumor remains. More work must be done on techniques that define a representative biopsy core for tumor length measurements, but some suggest that US-guided core biopsies for all prognostic markers already appear comparable to the surgical specimen (43). Finally, a new era of individual tumor markers is also beginning, such that tumor size criteria may not be as important for chemotherapy decisions, at least for estrogen-receptor-positive, node-negative patients (44–46). The absolute size of tumor foci within a tumor core relative to the actual specimen also raises the issue of the need for frequent repeat resection (47).

We did not see any local recurrences within a centimeter of the ablation zone for up to 6 years and treated one patient with new recurrences with a single repeat cryoablation session. Breast MR evaluation and careful preoperative planning likely accounted for our 100% short-term local control rate as much as our procedural success in achieving 1 cm visible ice margins that likely sculpted the cytotoxic ice beyond all tumor margins. The 93% accuracy of MR imaging in preoperative staging of breast cancer and its ability to markedly decrease positive surgical margins (12) also contributes to the high negative predictive value. Yet, we acknowledge that it may still appear difficult to compare our postablation MR follow-up to surgical specimen outcomes. Currently, if there is a positive surgical margin, residual tumor can be found at repeat resection in up to 50% of specimens (47). US guidance of lumpectomy localization may decrease the rate of positive surgical margins to ~11%, down from ~50%, for mammographically guided wire localization of breast cancers. Positive surgical margins could be decreased to as low as 5% if a freeze margin is extended more than 6 mm beyond the US-visible breast tumor and the ice-ball is resected in a procedure known as cryoassisted lumpectomy (48).

Careful MR evaluation and combined US- and CT-guided ablation could conceivably produce thorough tumor kill throughout an entire quadrant of a breast with good cosmetic outcome. In the near future, near-total cryomastectomy may also be possible with the advent of new cryotechnology that appears to be fivefold more powerful than current argon systems (49). Finally, advances in cryotechnology may also allow more interactive control and guidance with MR imaging, thereby allowing BC to be performed with the patient in the prone position, similar to current stereotactic and MR imaging-guided biopsies. This will better help volumetric comparisons of the ice ablation zone during the actual procedure with the pre-BC tumor volume and post-BC ablation zone coverage in follow-up.

Major weaknesses of our study arise from the limited patient group, which was self-selected and required vigilant skin protection that also dictated technique variability according to tumor size and location. Despite the apparent 100% procedural success with CT/US guidance, direct visual confirmation of visible ice 1 cm beyond tumor margins could only be done in fatty breast with CT. The use of US-visible adjacent landmarks to ensure 1-cm ice coverage beyond tumor margins still corresponded with thorough ablation zones at post-BC MR imaging follow-up. However, US guidance is still quite operator dependent and may be difficult to reproduce for most breast centers. In the future, greater accuracy and ease of use will be needed to ensure volumetric comparisons of (*a*) three-dimensional tumor locations; (*b*) the procedural ice extent, and (*c*) the subsequent ablation zone volume. This will likely require more sophisticated three-dimensional volume assessments (50) until breast MR imaging can more accurately guide the BC procedure and validate 1-cm ice extension beyond all tumor margins by using more reliable volumetric landmarks. For the unusual group of patients who chose cryoablation as an alternative to lumpectomy, none had complete axillary lymph node dissection to define nodal status. The first BC patient with multifocal cancer also did not agree to proceed with formal lymph node dissection after her

sentinel lymph node biopsy was positive for a minute focus of cancer. Several patients have reasoned that they were going on to radiation therapy and/or hormonal therapy anyway, so they simply wanted to avoid lymphedema morbidity that may accompany axillary dissection. The patient with bulky local recurrence and breast implants did have recurrence in an axillary node as well as in a site in the far upper breast, well beyond the original ablation site. However, she also remains without local recurrence anywhere in the breast following repeat cryoablation for the lower axillary node and the small satellite recurrence in the upper breast.

In summary, our limited breast cancer series suggests that BC can achieve thorough ablation for a broad range of tumor sizes and locations in safe, nearly pain-free outpatient procedures. Thorough evaluation of tumor extent and multiplicity with MR imaging enables cryoablation to be aggressively applied with multiple probes, which can produce thorough cytotoxic temperatures throughout even multifocal breast cancers by extending visible ice 1 cm beyond all visible tumor margins. Safety and excellent cosmesis appear possible with use of diligent skin protection techniques.

Acknowledgments

P.J.L. was a previous consultant for Endocare, Inc. While Endocare has sponsored previous clinical trials, this paper was entirely funded by internal funds of the cancer center, as part of the National Cancer Institute's Comprehensive Cancer Center Core Grant. P.J.L. is also an inventor and cofounder of cryotechnology of CryoDynamics LLC, which was not used in the course of this study. This study was partially supported by NIH Cancer Center Support grant CA-22453.

Abbreviations

BC	breast cryoablation
CTCAEv3	Common Toxicity Criteria for Adverse Events Version 3
DCIS	ductal carcinoma in situ

References

1. van Esser S, van den Bosch MA, van Diest PJ, Mali WT, Borel Rinkes IH, van Hillegersberg R. Minimally invasive ablative therapies for invasive breast carcinomas: an overview of current literature. World J Surg. 2007; 31:2284–2292. [PubMed: 17957404]
2. Huston TL, Simmons RM. Ablative therapies for the treatment of malignant diseases of the breast. Am J Surg. 2005; 189:694–701. [PubMed: 15910722]
3. Rubinsky B. Irreversible electroporation in medicine. Technol Cancer Res Treat. 2007; 6:255–260. [PubMed: 17668932]
4. Kaiser WA, Pfleiderer SO, Baltzer PA. MRI-guided interventions of the breast. J Magn Reson Imaging. 2008; 27:347–355. [PubMed: 18219688]
5. Lehman CD, Isaacs C, Schnall MD, et al. Cancer yield of mammography, MR, and US in high-risk women: prospective multi-institution breast cancer screening study. Radiology. 2007; 244:381–388. [PubMed: 17641362]
6. Saslow D, Boetes C, Burke W, et al. American Cancer Society guidelines for breast screening with MRI as an adjunct to mammography. CA Cancer J Clin. 2007; 57:75–89. [PubMed: 17392385]
7. Uematsu T, Yuen S, Kasami M, Uchida Y. Comparison of magnetic resonance imaging, multidetector row computed tomography, ultrasonography, and mammography for tumor extension of breast cancer. Breast Cancer Res Treat. 2008 Jan 12. Epub ahead of print.
8. Neubauer H, Li M, Kuehne-Heid R, Schneider A, Kaiser WA. High grade and non-high grade ductal carcinoma in situ on dynamic MR mammography: characteristic findings for signal increase and morphological pattern of enhancement. Br J Radiol. 2003; 76:3–12. [PubMed: 12595319]

9. Nielsen M, Thomsen JL, Primdahl S, et al. Breast cancer and atypia among young and middle-aged women: a study of 110 medicolegal autopsies. Br J Cancer. 1987; 56:814–819. [PubMed: 2829956]
10. Schnitt SJ, Silen W, Sadowsky NL, et al. Ductal carcinoma in situ (intraductal carcinoma) of the breast-current concepts. N Engl J Med. 1988; 318:898–903. [PubMed: 2832757]
11. Heywang-Köbrunner SH, Sinnatamby R, Lebeau A, Lebrecht A, Britton PD, Schreer I. Consensus Group. Interdisciplinary consensus on the uses and technique of MR-guided vacuum-assisted breast biopsy (VAB): results of a European consensus meeting. Eur J Radiol. 2008 Aug 22. Epub ahead of print.
12. Hollingsworth AB, Stough RG, O'Dell CA, Brekke CE. Breast magnetic resonance imaging for preoperative locoregional staging. Am J Surg. 2008; 196:389–397. [PubMed: 18436185]
13. Wiratkapun C, Duke D, Nordmann AS, et al. Indeterminate or suspicious breast lesions detected initially with MR imaging: value of MRI-directed breast ultrasound. Acad Radiol. 2008; 15:618–625. [PubMed: 18423319]
14. Genson CC, Blane CE, Helvie MA, Waits SA, Chenevert TL. Effects on breast MRI of artifacts caused by metallic tissue marker clips. AJR Am J Reontgenol. 2007; 188:372–376.
15. Permpongkosol S, Nicol TL, Khurana H, et al. Thermal maps around two adjacent cryoprobes creating overlapping ablations in porcine liver, lung and kidney. J Vasc Interv Radiol. 2007; 18:283–287. [PubMed: 17327563]
16. Rewcastle JC, Sandison GA, Muldrew K, Saliken JC, Donnelly BJ. A model for the time dependent three-dimensional thermal distribution within ice-balls surrounding multiple cryoprobes. Med Phys. 2001; 28:1125–1137. [PubMed: 11439482]
17. Bahn DK, Lee F, Badalament R, Kumar A, Greski J, Chernick M. Targeted cryoablation of the prostate: 7-year outcomes in the primary treatment of prostate cancer. Urology. 2002; 60(2 suppl 1):S3–S11.
18. Littrup P, Ahmed A, Aoun H, et al. CT- guided percutaneous cryotherapy of renal masses. J Vasc Interv Radiol. 2007; 18:383–392. [PubMed: 17377184]
19. Wang H, Littrup PJ, Duan Y, Zhang Y, Feng H, Nie Z. Thoracic masses treated with percutaneous cryotherapy: initial experience with more than 200 procedures. Radiology. 2005; 235:289–298. [PubMed: 15798173]
20. Allaf ME, Varkarakis IM, Bhayani SB, Inagaki T, Kavoussi LR, Solomon SB. Pain control requirements for percutaneous ablation of renal tumors: cryoablation versus radiofrequency ablation—initial observations. Radiology. 2005; 237:366–370. [PubMed: 16126920]
21. Tuncali K, Morrison PR, Winalski CS, et al. MRI-guided percutaneous cryotherapy for soft-tissue and bone metastases: initial experience. AJR Am J Reontgenol. 2007; 189:232–239.
22. Littrup PJ, Freeman-Gibb L, Andea A, et al. Cryotherapy for breast fibroadenomas. Radiology. 2005; 234:63–72. [PubMed: 15550369]
23. Kaufman CS, Littrup PJ, Freeman-Gibb LA, et al. Office-based cryoablation of breast fibroadenomas with long-term follow-up. Breast J. 2005; 11:344–350. [PubMed: 16174156]
24. Pfleiderer SO, Freesmeyer MG, Marx C, Kuhne-Heid R, Schneider A, Kaiser WA. Cryotherapy of breast cancer under ultrasound guidance: initial results and limitations. Eur Radiol. 2002; 12:3009–3014. [PubMed: 12439583]
25. Roubidoux MA, Sabel MS, Bailey JE, Kleer CG, Klein KA, Helvie MA. Small (<2. 0-cm) breast cancers: mammographic and US findings at US-guided cryoablation—initial experience. Radiology. 2004; 233:857–867. [PubMed: 15567802]
26. Pfleiderer SO, Marx C, Camara O, Gajda M, Kaiser WA. Ultrasound-guided, percutaneous cryotherapy of small (< or = 15 mm) breast cancers. Invest Radiol. 2005; 40:472– 477. [PubMed: 15973140]
27. Littrup PJ, Jallad B, Vorugu V, et al. Lethal isotherms of cryoablation in a phantom study: effects of heat load, probe size and number. J Vasc Interv Radiol. 2009 (in press).
28. Evans W, Fish J, Keblinski P. Thermal conductivity of ordered molecular water. J Chem Phys. 2007; 126:154–504.
29. Trotti A, Colevas AD, Setser A, et al. CTCAE v3. 0: development of a comprehensive grading system for the adverse effects of cancer treatment. Semin Radiat Oncol. 2003; 13:176–181. [PubMed: 12903007]

30. Sacks D, McClenny TE, Cardella JF, Lewis CA. Society of Interventional Radiology clinical practice guidelines. J Vasc Interv Radiol. 2003; 14:S199–S202. [PubMed: 14514818]
31. Goldberg SN, Grassi CJ, Cardella JF, et al. Image-guided tumor ablation: standardization of terminology and reporting criteria. J Vasc Interv Radiol. 2005; 16:765–778. [PubMed: 15947040]
32. Rand RW, Rand RP, Eggerding FA, et al. Cryolumpectomy for breast cancer: an experimental study. Cryobiology. 1985; 22:307–318. [PubMed: 2992882]
33. Hong JS, Rubinsky B. Patterns of ice formation in normal and malignant breast tissue. Cryobiology. 1994; 31:109–120. [PubMed: 8004992]
34. Staren ED, Sabel MS, Gianakakis LM, et al. Cryosurgery of breast cancer. Arch Surg. 1997; 132:28–33. discussion 34. [PubMed: 9006549]
35. Rui J, Tatsutani KN, Dahiya R, Rubinsky B. Effect of thermal variables on human breast cancer in cryosurgery. Breast Cancer Res Treat. 1999; 53:185–192. [PubMed: 10326796]
36. Susini T, Nori J, Olivieri S, et al. Radiofrequency ablation for minimally invasive treatment of breast carcinoma. a pilot study in elderly inoperable patients. Gynecol Oncol. 2007; 104:304–310. [PubMed: 17070572]
37. Khatri VP, McGahan JP, Ramsamooj R, et al. A phase II trial of image-guided radiofrequency ablation of small invasive breast carcinomas: use of saline-cooled tip electrode. Ann Surg Oncol. 2007; 14:1644–1652. [PubMed: 17508251]
38. Garbay JR, Mathieu MC, Lamuraglia M, Lassau N, Balleyguier C, Rouzier R. Radiofrequency thermal ablation of breast cancer local recurrence: a phase II clinical trial. Ann Surg Oncol. 2008 Aug 15. Epub ahead of print.
39. White RL Jr. Cryoablative therapy in breast cancer: no. J Surg Oncol. 2008; 97:483–484. [PubMed: 18425784]
40. Yeap BH, Muniandy S, Lee SK, Sabaratnam S, Singh M. Specimen shrinkage and its influence on margin assessment in breast cancer. Asian J Surg. 2007; 30:183–187. [PubMed: 17638637]
41. Pritt B, Tessitore J, Weaver D, Blaszyk H. The effect of tissue fixation and processing on breast cancer size. Hum Pathol. 2005; 36:756–760. [PubMed: 16084944]
42. Yang JH, Lee WS, Kim SW, Woo SU, Kim JH, Nam SJ. Effect of core-needle biopsy vs fine-needle aspiration on pathologic measurement of tumor size in breast cancer. Arch Surg. 2005; 140:125–128. [PubMed: 15723992]
43. Ozdemir A, Voyvoda NK, Gultekin S, Tuncbilek I, Dursun A, Yamac D. Can core biopsy be used instead of surgical biopsy in the diagnosis and prognostic factor analysis of breast carcinoma? Clin Breast Cancer. 2007; 7:791–795. [PubMed: 18021481]
44. Flanagan MB, Dabbs DJ, Brufsky AM, Beriwal S, Bhargava R. Histopathologic variables predict Oncotype DX Recurrence Score. Mod Pathol. 2008 Mar 21. Epub ahead of print.
45. Habel LA, Shak S, Jacobs MK, et al. A population-based study of tumor gene expression and risk of breast cancer death among lymph node-negative patients. Breast Cancer Res. 2006; 8:R25. Epub 2006 May 31. [PubMed: 16737553]
46. Conlin AK, Seidman AD. Use of the Oncotype DX 21-gene assay to guide adjuvant decision making in early-stage breast cancer. Mol Diagn Ther. 2007; 11:355–360. [PubMed: 18078353]
47. Miller AR, Brandao G, Prihoda TJ, et al. Positive margins following surgical resection of breast carcinoma: analysis of pathologic correlates. J Surg Oncol. 2004; 86:134–140. [PubMed: 15170651]
48. Tafra L, Smith SJ, Woodward JE, Fernandez KL, Sawyer KT, Grenko RT. Pilot trial of cryoprobe-assisted breast-conserving surgery for small ultrasound-visible cancers. Ann Surg Oncol. 2003; 10:1018–1024. [PubMed: 14597439]
49. Littrup, PJ.; Babkin, AV.; Duncan, RV.; Boldarev, S., inventors. CryoDynamics LLC, assignee. Methods and systems for cryogenic cooling. US patent. 7,273,479. Sep 25. 2007
50. Zou KH, Tuncali K, Warfield SK, et al. Three-dimensional assessment of MR imaging-guided percutaneous cryotherapy using multi-performer repeated segmentations: the value of supervised learning. Acad Radiol. 2005; 12:444–450. [PubMed: 15831417]

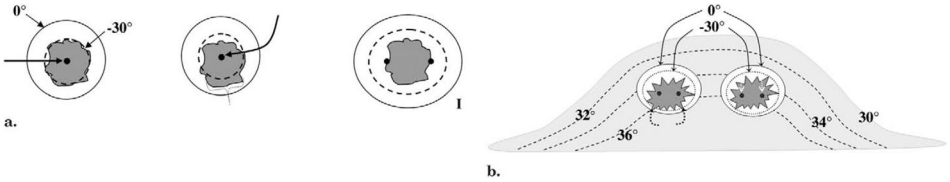

Figure 1.

(a) Diagram shows basic isotherms for single and double cryoprobes. Accurate central placement of a single 2.4-mm cryoprobe (left image, arrow) within a simulated 1.2 × 1.2-cm tumor (dark gray) may still not produce sufficient lethal ice to cover all tumor margins (dashed line ~ <−30°C, diameter ~ 1.2 cm). Even though visible ice (solid outer line) may appear to cover all tumor margins, slight off-center placement (middle image, arrow) leaves grossly untreated tumor (bracket) beyond the lethal isotherm (dashed line). Tumor on right is covered by lethal ice due to synergy produced by two cryoprobes (15). ***(b)*** *Avoiding posterior positive margins:* heat load effects of the chest wall. The estimated temperature difference between skin surface (30°C) and chest wall/body (36°C) causes greater heat load along the posterior margin of ice propagation, which narrows the posterior distance between the visible (0°C) and lethal (–30°C) isotherms (curved solid arrows). Ablation on left shows central position of cryoprobes and greater anterior extension of visible ice beyond tumor margin; however, incomplete coverage of posterior tumor margins (black dashed arrows) is noted, similar to that seen in prior series (24–26). Ablation on right shows through tumor coverage by lethal ice due to more posterior placement of cryoprobes in tumor (white straight arrows), thus overcoming heat-sink effect along the chest wall.

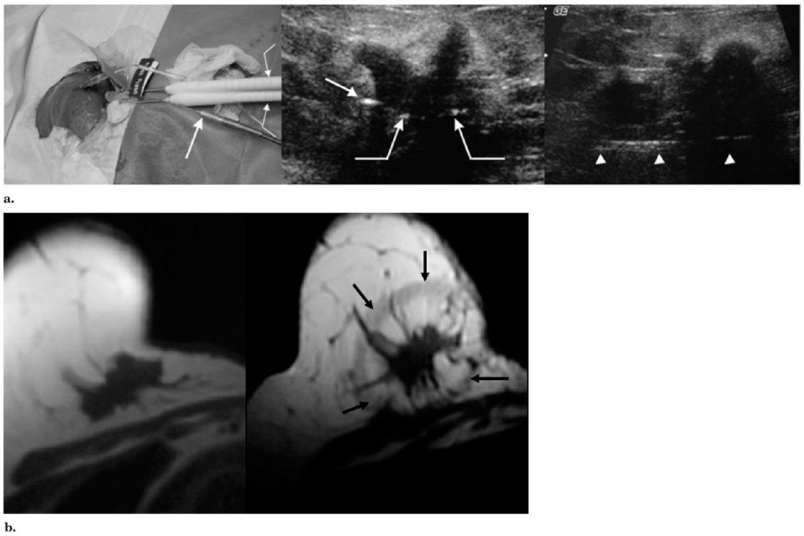

Figure 2.

(a) US- guided cryotherapy for local control. Left image, BC performed with two cryoprobes (curved arrow) and a thermocouple (straight arrow) for an irregular 2.0-cm mass using technique planning noted in Figure 1b for tumors closer to the chest wall. As this was our second patient, this procedure also highlighted the need for better circumferential posterior visualization of the iceball near the chest wall, which was better provided with CT guidance. Middle image, Axial US image through the largest portion of the irregular mass shows more posterior placements of cryotherapy probes (curved arrows) and cross-section of a thermocouple en route to the superior tumor (straight arrow). Despite the cancer being near the chest wall, its medial location gave it a relatively superficial position for good US visualization. Right image, sagittal US image shows the posterior course of a thermocouple, which measured −57°C after ~8 minutes of the second freeze cycle at the superior tumor margin. The mobile nature of this tumor allowed substantial retraction off the chest wall in addition to saline injection. **(b)** MR images obtained before and four weeks after cryotherapy for local control. Left image, axial T1-weighted MR image obtained before cryotherapy at a similar tumor level as in Figure 2a. The tumor is causing retraction but does not involve the skin. Right image, MR image obtained four weeks after cryotherapy shows a low-signal-intensity rim of edema (black arrows) surrounding an ovoid zone of avascular necrosis that extended approximately 1 cm beyond all visible tumor margins but without extension into the chest wall. The wheelchair-bound patient, who was not a candidate for surgery, continued to do well with tumor involution of the primary and no further progression of distant metastases on anastrozole (Arimidex; AstraZeneca Pharmaceuticals, Delaware City, Delaware) alone until her death two years later.

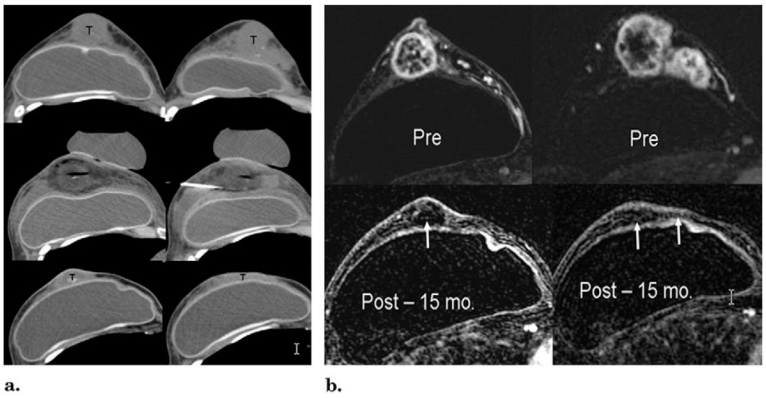

a. b.

Figure 3.

(a) CT guidance before and after cryotherapy. Top images, unenhanced CT images at the level of the nipple and superior breast show extensive tumor involvement (*T*). The skin and tumor appear inseparable but were NOT fixed at physical examination or involved at US or MR imaging (Fig 5b). Middle images, CT images at the same levels immediately after cryotherapy and probe removal, leaving air in tracts. The tumors are covered by hypodense ice, except for the image on right, where the ice had already melted after cryoprobes had been retracted from an earlier medial freeze cycle. The saline injection needle remains between the tumor and the implant and skin had also been infiltrated. Bottom images, CT images obtained at the same anatomic levels 15 months after cryotherapy show marked resolution of prior bulky tumors. Random biopsies performed six weeks after ablation showed no residual tumor (*T*), but cancer recurred in two sites beyond the ablation zone at seven months. Repeat cryotherapy was done for a 6-mm new nodule in the far upper central breast and a 17-mm lower axillary node. **(b)** MR evaluation before (*Pre*) and 15 months after (*Post*) cryotherapy. Top images, before cryotherapy, T1-weighted fat-suppressed gadolinium-enhanced axial MR images show brisk enhancement throughout the tumor nodularity of the retroareolar (left) and superior (right) breast. Note also the lack of skin enhancement. Bottom images, T1-weighted fat-suppressed gadolinium-enhanced MR images obtained at the same levels 15 months after cryotherapy show a marked reduction of prior bulky tumors and no residual enhancement of any margin (arrows).

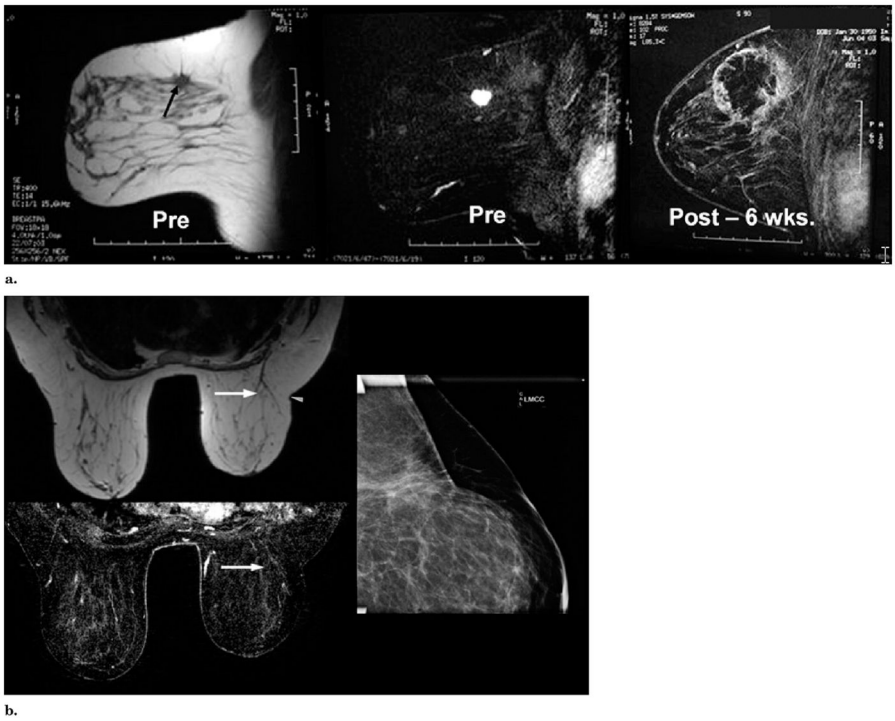

Figure 4.

(a) MR images obtained before (*Pre*) and six weeks after (*Post*) cryotherapy of multifocal left upper outer quadrant cancer. Left image, T1-weighted axial image shows the spiculated, 1.6-cm dominant mass in the left outer quadrant (arrow). Another biopsy-confirmed cancer in the same quadrant was seen in different image planes. Middle image, fat-subtracted T1-weighted image obtained after the administration of gadolinium shows brisk tumor enhancement. Right image, T1-weighted, fat-subtracted, gadolinium-enhanced MR image obtained six weeks after cryotherapy shows a rim of enhancement corresponding to a healing cryotherapy rim, which also covered the other cancer. The microlumpectomy sampling (ie, Mammotome removal) of the tumor region before initiation of the freeze made our first BC procedure more complex. US visualization of the tumor site became distorted by blood during the vacuum-assisted biopsies, which are no longer used. Despite poor visualization of any remaining tumor margin, thorough ablation margins were still achieved by placing the cryoprobes along the outer margins of these microlumpectomy sites. Biopsy of three slightly nodular areas of rim enhancement showed no residual cancer or DCIS. **(b)** Images obtained at five-year follow-up. Top left image, T1-weighted axial MR image shows minimal scarring and/or distortion at the cryosite (arrow). Slightly smaller left breast was initially present and lateral scar indentation (arrowhead) is a scar from abscess débridement performed one year before this study (ie, four years after cryotherapy), which also confirmed no residual tumor throughout the original cryotherapy site. Bottom left image, T1-weighted fat-subtracted, gadolinium-enhanced MR image shows no enhancement of the previous ablation and subsequent resection sites (arrow). Right image, compression mammogram of the left upper outer quadrant shows no mass effect and minimal scarring, likely related to resection one year ago rather than original cryotherapy five years ago.

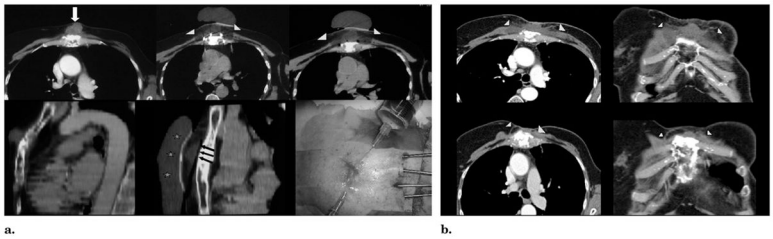

Figure 5.

(a) Chest wall cryotherapy for bone metastasis about to break through skin. The patient was a 68-year-old woman with continuously growing sternal and soft tissue tumor but was otherwise stable. Results of positron emission tomography (PET) were negative for bone metastases from breast cancer. There was only a very thin layer of intact movable skin overlying the tumor. The top axial images show the 4.7 × 3.8 × 4.0-cm enhancing tumor (arrow), then covered in ice (arrowheads) extending to the skin surface. Bottom row shows sagittal reconstructions before (left) and during cryotherapy (middle), noting tumor (black arrows) covered by ice and warmed saline bags on skin (stars). Bottom right procedure image shows four cryoprobes and two skin injection sites. **(b)** Chest wall cryotherapy—follow-up. The hypovascular zone one month after BC (top row, arrowheads) corresponded to the visible ice extent 1 cm beyond the lateral tumor margins. Enhanced axial and coronal CT images obtained 18 months after BC (bottom row) show near-complete resorption of tumor mass with good remodeling of adjacent normal tissues (arrowheads). This area also remained negative at PET and bone scanning performed at 36 months, with no other distant disease recurrences.

Table

Summary of Tumor Sizes and Treatment Parameters

Patient			Guidance		Tumor				Follow-up (mo)		Biopsy			
TMN Stage/Clinical Stage	Selection Criteria	Patient (No.), Tumor (a–e)	US	CT	No.	Size (mm)*	No. of Probes Used	Ice (mm)*	Clinical	Imaging	Sentinal Lymph Node Biopsy	Preprocedure	During the Procedure	Postprocedure
T2N1M0/IIA	New Dx	1a	✓		1 of 2	13 × 9 × 8	3	60 × 30 × 50	72	72		✓	✓	✓
		1b	✓		2 of 2	10 × 8 × 21		One iceball			✓	✓	✓	
T3N2M0/IIIA	Recurrent	2	✓		1	19 × 24 × 45	2	43 × 53 × 48	7	1				
T1cN0M0/I	New Dx	3a	✓		1 of 2	15 × 14 × 20	3	100 × 40 × 100	30	29	✓		✓	
		3b	✓		2 of 2	20 × 19 × 18		One iceball					✓	
T3N2M1/IV	Recurrent	4a	✓	✓	1 of 2	58 × 33 × 65	7	82 × 43 × 75	30	24				✓
		4b	✓	✓	2 of 2	Node: 18 × 11 × 18	2	30 × 25 × 45						
T3N2M1/IV	Recurrent	4c	✓	✓	1 of 2	6 × 4 × 8	2	25 × 20 × 30	17	17		✓		
		4d	✓	✓	2 of 2	Node: 17 × 12 × 21	2	33 × 25 × 36				✓		
T3N2M1/IV	New Dx	5	✓		1	14 × 9 × 15	3	70 × 30 × 80	24	1			✓	
T3N2M1/IV	New Dx	6	✓		1	15 × 14 × 14	2	42 × 27 × 46	17	1	✓	✓	✓	
TxN0M1/IV	Recurrent	7	✓	✓	1	27 × 15 × 25	3**	46 × 39 × 45	18	11			✓	
TxN1M1/IV	Recurrent	8	✓	✓	1	47 × 38 × 40	4	80 × 47 × 74	38	38		✓		
T2N1M0/IIB	Recurrent	9a	✓		1 of 5	20 × 17 × 20	5	100 × 43 × 100	9	9		✓		
		9b	✓		2 of 5	6 × 7 × 6		One iceball						
		9c	✓		3 of 5	5 × 5 × 5								
		9d	✓		4 of 5	5 × 5 × 5								
		9e	✓		5 of 5	Node: 12 × 14 × 15								
T1N1M0/IIB	New Dx	10	✓	✓	1 of 2	14 × 19 × 15	2	44 × 32 × 35	5	1		✓		
			✓	✓	2 of 2	Node: 12 × 6 × 14		52 × 30 × 35						
T2N1M0/IIB	New Dx	11	✓	✓	1 of 2	20 × 19 × 20	4	70 × 50 × 60	6	6	✓	✓	✓	
			✓	✓	2 of 2	12 × 11 × 11		One iceball						
Sum/Averages	**6 new Dx 5 recurrent**				**22**	**16.9 mm**	**3.1**	**50.7 mm**	**22.8**	**17.5**	**4**	**9**	**8**	**2**

Note.—Dx = newly diagnosed breast cancer. 100% technical success in covering all tumor margins by 1 cm visible ice is a subjective criteria, but can still be inferred by noting that tumors averaging nearly 2 cm were treated with an average of three cryoprobes and caused 5-cm ablation zones (ie, 1.5-cm ice margins = [5 – 2]/3).

* Measurements are given in transverse × anteroposterior × craniocaudal dimensions.

** Used 1.7-mm diameter cryoprobes; all others were 2.4 mm.